Ab Initio Ionization and Excitation Spectra Involving IO($X^2\Pi$) and IO^+($X^3\Sigma^-$, $a^1\Delta$, $b^1\Sigma^+$)

Parviz Hassanzadeh, Karl K. Irikura,* and Russell D. Johnson, III

Physical and Chemical Properties Division, National Institute of Standards and Technology, Gaithersburg, Maryland 20899

Received: March 20, 1997; In Final Form: June 24, 1997[⊗]

An equilibrium bond length of $r_e = 1.894$ Å and harmonic vibrational frequency of $\omega_e = 664$ cm^{-1} are computed for IO($X^2\Pi$) at the nonrelativistic all-electron CCSD(T)/6-311+G(3df) level of theory. These are within 1% of the experimental Ω-averaged values of 1.877 ± 0.005 Å (3σ) and 670 ± 13 cm^{-1} (3σ), respectively. Similar calculations predict $r_e = 1.824$ Å and $\omega_e = 764$ cm^{-1} for IO^+ ($X^3\Sigma^-$). For the singlet excited electronic states of IO^+, which require a multireference treatment, CASPT2(8,6)/6-311+G(3df) predicts $r_e = 1.841$ Å and $\omega_e = 738$ cm^{-1} for IO^+($a^1\Delta$) and $r_e = 1.870$ Å and $\omega_e = 679$ cm^{-1} for IO^+($b^1\Sigma^+$). The equilibrium bond length increases and the harmonic vibrational frequency decreases from the ground to the excited states of IO^+ as observed for the isovalent O_2 molecule. A spin−spin splitting of 1060 ± 160 cm^{-1} (3σ) is assigned to the two sublevels of the ground state of iodine monoxide cation, IO^+ ($X_1{}^3\Sigma^-{}_0$, $X_2{}^3\Sigma^-{}_{\pm1}$), on the basis of a reinterpretation of an experimental photoionization efficiency spectrum of IO. This reassignment is required by the present vibrational constants for IO^+, Franck−Condon factors, and four-component, relativistic multireference configuration interaction (CI) calculations of the spin−spin splitting. An adiabatic ionization energy of 9.60 eV is computed at the CCSD(T) level of theory for the $IO^+(X^3\Sigma^-{}_0) \leftarrow IO(X^2\Pi_{3/2})$ transition and is in reasonable agreement with the experimental photo-ionization threshold of 9.735 ± 0.017 eV (3σ). Adiabatic excitation energies of 0.72 and 1.18 eV are calculated at the CASPT2 level of theory for $IO^+(a^1\Delta) \leftarrow IO^+(X^3\Sigma^-{}_0)$ and $IO^+(b^1\Sigma^+) \leftarrow IO^+(X^3\Sigma^-{}_0)$ transitions, respectively. The photoionization spectrum of IO and excitation spectrum of IO^+ have also been simulated.

1. Introduction

Halogen monoxides have been implicated as effective catalysts in destroying ozone in the atmosphere.[1] Chlorine and bromine monoxides are important in the stratosphere while iodine monoxide is mostly restricted to the troposphere[2] as a result of the photolytic instability of iodine-containing species.[3]

The ionization energy of iodine monoxide has recently been measured by vacuum−ultraviolet (VUV) photoionization mass spectrometry.[4] However, the spectrum is congested and its interpretation somewhat tentative. This work is an attempt to shed some light on this matter by predicting the ionization energies of IO and the excitation energies and molecular constants for IO^+. The molecular constants are also required to derive temperature-dependent thermochemistry.[5]

2. Methods

Potential energy curves for the ground states of IO($X^2\Pi$) , IO^+($X^3\Sigma^-$), and O_2 ($X^3\Sigma^-$) were computed at the CCSD(T) level[6−8] (coupled cluster with all single and double substitutions and a quasi-perturbative estimate of triple excitations). The equilibrium bond distance for IO($X^2\Pi$) was also computed at the QCISD(T) level[9−11] (quadratic configuration interaction with all single and double substitutions and a quasi-perturbative estimate of triple excitations). The potential energy curves for these states and the excited states of IO^+ and O_2, which have multiconfiguration nature, were also computed at the CASPT2 level[12] (complete active space self-consistent field with dynamic correlation from second-order perturbation theory). The active electrons and space in the CASPT2 calculations for IO($X^2\Pi$) consist of the valence $(\sigma_p)^2$, $(\pi_p)^4$, $(\pi^*_p)^3$, and $(\sigma^*_p)^0$ orbitals, denoted CASPT2(9,6). For IO^+($X^3\Sigma^-$, $a^1\Delta$, $b^1\Sigma^+$) and O_2 ($X^3\Sigma^-_g$, $a^1\Delta_g$, $b^1\Sigma^+_g$), there are only eight valence p electrons and the corresponding calculation is CASPT2(8,6). All single reference calculations were spin unrestricted.

The segmented 6-311+G(3df) basis set for O was taken from the Gaussian 94 program,[13,14] and the basis set for I was that developed by McGrath and Radom for Gaussian 2 (G2) energy calculations,[15] except that a splitting ratio of 4/1/0.25 was used for the polarizing d-functions. The iodine basis set is contracted as (16,14,8,1)/[9,8,5,1] or more explicitly as (631 111 111, 33 311 111, 41 111, 1). Sadlej's generally-contracted polarized basis sets (PBSs)[16−18] for O and I were used as supplied with the MOLCAS-3 program.[19,14] Another slightly modified basis set for O was prepared by uncontracting the most diffuse d-type function and adding an uncontracted f-type function ($\alpha_f = 1.334$) and may be represented as (10,6,4,1)/[5,3,3,1] or (52 111, 411, 211, 1). The small oxygen atomic-natural-orbital (ANO) basis sets as supplied with the MOLCAS-3 programs[19,14] were also used for O_2.

The MOLCAS-3 programs[19,14] were used to compute CASPT2 energies and molecular spectroscopic constants. The MOLCAS-3 calculations were run on an IBM RS-6000/590 computer, and the CCSD(T) and QCISD(T) calculations were done using the ACES II[20,21] and Gaussian 94[13] programs running on Cray C-90 and IBM RS-6000/590 computers.[14] The relativistic calculations were carried out using the MOLFDIR program suite[22,23] running on a Cray C-90.[14]

3. Results

The basis set quality, level of calculation, and size of active space in the multiconfiguration calculations were tested for O_2 (isovalent with IO^+) and IO, for which the molecular constants are known experimentally. For this purpose the calculated and the experimental excitation energy (T_e), internuclear distance (r_e), and Dunham coefficients through second order were examined: harmonic vibrational frequency ($\omega_e = Y_{10}$), vibra-

[⊗] Abstract published in *Advance ACS Abstracts,* August 15, 1997.

S1089-5639(97)01007-4 CCC: $14.00

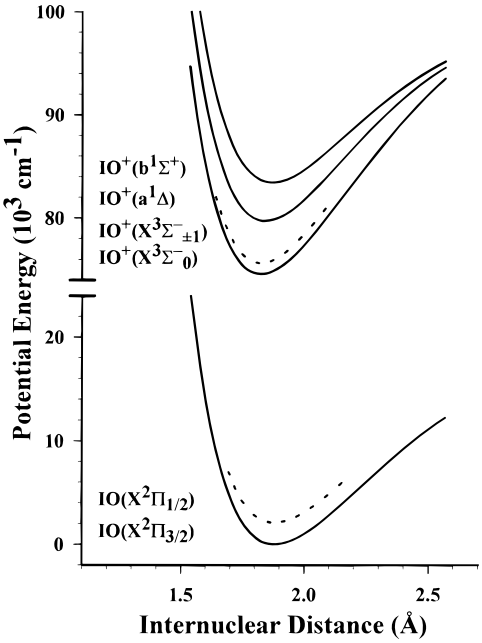

Figure 1. CASPT2 potential energy curves for IO(X $^2\Pi_{3/2}$) and IO$^+$(X $^3\Sigma^-_0$, a$^1\Delta$, b$^1\Sigma^+$). The dashed curves represent the upper sublevels IO(X $^2\Pi_{1/2}$) and IO$^+$(X$^3\Sigma^-_{\pm1}$).

tional anharmonicity ($\omega_e x_e = -Y_{20}$), rotational constant ($B_e = Y_{01}$), second-order rotational constant ($D_e = -Y_{02}$), and vibration−rotation constant ($\alpha_e = -Y_{11}$). Unless otherwise indicated, the dynamic electron correlation calculations in the following discussion were performed with the valence and 4d orbitals active and the core frozen.

3.1. Potential Energy Curves. *O_2.* The electronic energies for O_2(X$^3\Sigma^-_g$, a$^1\Delta_g$, b$^1\Sigma^+_g$) were calculated at bond lengths ranging from 0.95 to 2.0 Å at 0.025 Å intervals using the 6-311+G(3df), ANO, and PBS basis sets. The CASPT2(8,6) and CCSD(T) levels of theory were used for X$^3\Sigma^-_g$ and the CASPT2(8,6) level for the singlet states. These calculations were performed both (1) with all electrons active and (2) with only valence electrons active in the treatment of dynamic electron correlation. As expected, the CASSCF calculations revealed that the ground state is dominated by a single determinant around the equilibrium bond length (r_e), whereas each of the excited states a$^1\Delta$ and b$^1\Sigma^+$ is dominated by two equally weighted configurations.

IO. Electronic energies for bond lengths ranging from 1.5 to 2.6 Å at 0.025 Å intervals were computed at the CASPT2(9,6) level using the 6-311+G(3df) and PBS basis sets. IO(X$^2\Pi$) is dominated by a single configuration. For comparison, the potential energy curve (r = 1.5−2.2 Å) was also calculated at the CCSD(T)/6-311+G(3df) level. CCSD(T) energies at $r >$ 2.2 Å were discarded due to severe spin contamination, which was manifested as a discontinuity in the potential curve.

IO^+. The potential energy curves for IO$^+$(X $^3\Sigma^-$, a$^1\Delta$, b$^1\Sigma^+$) (r = 1.5−2.2 Å) were computed at the CASPT2(8,6)/6-311+G(3df) level. As for O_2, the ground state is single configuration but the singlet excited states are dominated by two equally weighted configurations. The potential energy curve for the ground state was also scanned at the CCSD(T)/6-311+G(3df) level.

The CASPT2/6-311+G(3df) potential energy curves for IO(X $^2\Pi_{3/2}$) and IO$^+$(X$^3\Sigma^-_0$, a$^1\Delta$, b$^1\Sigma^+$) are shown as the solid curves in Figure 1. The curves for the ground sublevels of the neutral and cation were obtained by correcting the calculated, Ω-averaged curves by the experimental spin−orbit and spin−spin splittings at r_0. The upper sublevels, calculated similarly, are shown as dashed curves.

3.2. Molecular Constants and Spectra. Equilibrium bond lengths and ro-vibrational constants for each of the states were calculated by numerical solution of the ro-vibrational Schrödinger equation as implemented in the VIBROT program of the MOLCAS-3 suite.[19,14] Seven vibrational and four rotational quantum levels were calculated, and the molecular constants for each state were derived by fitting these levels to the formulas shown in Tables 1−3. The molecular constants calculated from the CASPT2 and CCSD(T) potential curves are shown in Tables 1, 2, and 3 for O_2, IO, and IO^+, respectively. The experimental values for O_2 and IO are also included in these Tables. The Franck−Condon factors for the ionization of IO(X$^2\Pi$) to the IO$^+$(X$^3\Sigma^-$, a$^1\Delta$, b$^1\Sigma^+$) states and for the excitation of IO$^+$(X$^3\Sigma^-$) to the IO$^+$(a$^1\Delta$, b$^1\Sigma^+$) states were computed using the corresponding vibrational wave functions and are shown in Table 4.

The CASPT2 and CCSD(T) calculations do not include spin−orbit or spin−spin interactions for IO(X$^2\Pi$) and IO$^+$(X$^3\Sigma^-$). These effects were added as corrections using the experimental spin−orbit splitting of 2091 ± 40 cm^{-1} (1σ) for IO(X$^2\Pi$)[24,25] and a spin−spin splitting of 1060 ± 160 cm^{-1} (3σ) for IO$^+$(X$^3\Sigma^-$). The latter value was derived from the experimental photoionization spectrum[4] as discussed in the next section. The excitation and ionization energies, corrected for the spin-coupling effects and zero-point vibrational energy differences, are summarized in Table 5. The calculated spectrum for the ionization of the IO(X $^2\Pi_{3/2}$) to the IO$^+$(X $^3\Sigma^-_0$, X $^3\Sigma^-_{\pm1}$, a$^1\Delta$, b$^1\Sigma^+$) states, as convoluted with a gaussian line shape with a spectral bandwidth (FWHM) of 0.02 eV, is shown in Figure 2. For the figure, ionizations to IO$^+$(X$^3\Sigma^-$, a$^1\Delta$, b$^1\Sigma^+$) were arbitrarily assumed to be equally likely. The absolute magnitudes of the Franck−Condon factors calculated for the IO$^+$(X $^3\Sigma^-$) ← IO(X $^2\Pi_{3/2}$) transitions are distributed over the X$^3\Sigma^-_0$ and X$^3\Sigma^-_{\pm1}$ sublevels, which have been assigned the statistical ratio of 1:2. The hot bands ($v'' = 1$) are populated with less than 3% at 300 K but are included in Figure 2 (lower axis). The Franck−Condon factors for the transitions from IO($v'' =$ 0) to IO$^+$($v' = 0$) are larger than those to IO$^+$($v' = 1$) by factors of 2, 4, and 50 for the X$^3\Sigma^-$, a$^1\Delta$, and b$^1\Sigma^+$ states, respectively (Figure 2).

The spectrum for electronic transitions from IO$^+$(X$^3\Sigma^-_0$) to IO$^+$(a$^1\Delta$, b$^1\Sigma^+$), also simulated with a gaussian bandwidth of 0.02 eV, is shown in Figure 3. Transitions to the upper states were arbitrarily assumed to be equally likely. The Franck−Condon factors for the transitions from X$^3\Sigma^-_0$($v'' = 0$) to a $^1\Delta$(v' = 0) and b$^1\Sigma^+$($v' = 0$) are larger than those to $v' = 1$ by factors of 20 and 3, respectively.

3.3. Spin−Spin Splitting. The spin−spin splitting ($2\lambda_e$) between the Ω = 0 and Ω = ±1 sublevels in IO$^+$ (X$^3\Sigma^-$) was estimated using a relativistic, four-component, multireference configuration interaction calculation. The electron−electron Hamiltonian included the Coulombic and magnetic Gaunt interactions. We used a bond length of 1.8245 Å. The frozen-core MRCI was of the RASCI type,[26] with four spinors (valence s) in the RAS1 space, 12 in the RAS2 space (valence p), and all the remaining virtuals in the RAS3 space. The reference space thus consisted of the full CI within RAS2, or complete open-shell CI (8 electrons in 12 spinors).[27] The reference COSCI (495 determinants) yielded $2\lambda_e$ = 918 cm^{-1}. RASCI adds all single and double excitations from RAS1 and all single and double excitations into RAS3 (2×10^6 determinants in each relevant symmetry block) and yielded $2\lambda_e$ = 892 cm^{-1}. Averaged orbitals (2 electrons in 4 spinors) were used for the

TABLE 1: Comparison of Calculated and Experimental Molecular Constants[a] for the Ground and Excited States of O_2[b]

$^{16}O_2$	state	T_e	ω_e	$\omega_e x_e$	B_e	$\alpha_e/10^{-2}$	$D_e/10^{-6}$	r_e
exptl[c]	$X^3\Sigma^-_g$	0	1580.193	11.981	1.44563	1.593	4.839	1.20752
CASPT2(8,6)	$X^3\Sigma^-_g$	0	1585	12.04	1.441	1.57	4.81	1.2095
CCSD(T)	$X^3\Sigma^-_g$	0	1606	11.25	1.444	1.51	4.67	1.2082
exptl[c]	$a^1\Delta_g$	7918.1	1509.8	12.90[d]	1.4264	1.71	4.86	1.21563
CASPT2(8,6)	$a^1\Delta_g$	8162	1514	14.41	1.422	1.705	5.00	1.2176
exptl[c]	$b^1\Sigma^+_g$	13195.1	1432.77	14.00	1.40037	1.82	5.351	1.22688
CASPT2(8,6)	$b^1\Sigma^+_g$	13825	1425	14.63	1.394	1.84	5.31	1.2296

[a] $G(v) = \omega_e(v + 1/2) - \omega_e x_e(v + 1/2)^2 + \omega_e y_e(v + 1/2)^3$, $F_v(J) = B_v J(J + 1) - D_v J^2(J + 1)^2$, $B_v = B_e - \alpha_e(v + 1/2) + \gamma_e(v + 1/2)^2$, $D_v = D_e + \beta_e(v + 1/2)$. $\omega_e y_e$, γ_e, and β_e are very sensitive to errors in the potential curves and are not included in the table. [b] All values are in cm^{-1} except for r_e, which is in angstroms. Calculations are with the 6-311+G(3df) basis set and frozen core. [c] Reference 28. [d] Estimated.

TABLE 2: Comparison of Calculated and Experimental Molecular Constants[a] for the Ground State of IO[b]

$^{127}I^{16}O$	state	ω_e	$\omega_e x_e$	B_e	$\alpha_e/10^{-3}$	$D_e/10^{-7}$	r_e
exptl[c]	$X^2\Pi_{3/2}$	681.6004(91)	4.3699(30)	0.34021(2)	2.71(3)	3.5(2)	1.867713(46)
exptl[d]	$X^2\Pi_{1/2}$	658(25)					1.887(10)
CASPT2(9,6)	$X^2\Pi$	652	4.76	0.336	3.3	3.55	1.8799
CCSD(T)	$X^2\Pi$	664	3.7	0.331	2.6	3.30	1.8939

[a] $G(v) = \omega_e(v + 1/2) - \omega_e x_e(v + 1/2)^2 + \omega_e y_e(v + 1/2)^3$, $F_v(J) = B_v J(J + 1) - D_v J^2(J + 1)^2$, $B_v = B_e - \alpha_e(v + 1/2) + \gamma_e(v + 1/2)^2$, $D_v = D_e + \beta_e(v + 1/2)$. $\omega_e y_e$, γ_e, and β_e are very sensitive to errors in the potential curves and are not included in the table. [b] All values are in cm^{-1} except for r_e, which is in angstroms. Calculations are with the 6-311+G(3df) basis set and frozen core. [c] Reference 31. Uncertainties are 3σ. [d] References 24 and 25.

TABLE 3: Calculated Molecular Constants[a] for the Ground and Excited States of IO^+[b]

$^{127}I^{16}O^+$	state	T_e[c]	ω_e	$\omega_e x_e$	B_e	$\alpha_e/10^{-3}$	$D_e/10^{-7}$	r_e
CASPT2(8,6)	$X^3\Sigma^-$	0	779	5.79	0.357	2.7	2.99	1.8238
CCSD(T)	$X^3\Sigma^-$	0	764	8.16	0.357	3.7	3.23	1.8244
CASPT2(8,6)	$a^1\Delta$	5790	738	5.54	0.350	2.9	3.15	1.8413
CASPT2(8,6)	$b^1\Sigma^+$	9494	679	5.72	0.340	3.1	3.38	1.8695

[a] $G(v) = \omega_e(v + 1/2) - \omega_e x_e(v + 1/2)^2 + \omega_e y_e(v + 1/2)^3$, $F_v(J) = B_v J(J + 1) - D_v J^2(J + 1)^2$, $B_v = B_e - \alpha_e(v + 1/2) + \gamma_e(v + 1/2)^2$, $D_v = D_e + \beta_e(v + 1/2)$. $\omega_e y_e$, γ_e, and β_e are very sensitive to errors in the potential curves and are not included in the table. [b] All values are in cm^{-1} except for r_e, which is in angstroms. The calculations are with the 6-311+G(3df) basis set and frozen core. [c] Using a spin−spin splitting of 1060 ± 160 cm^{-1} derived from data in ref 4 (see text).

TABLE 4: Franck−Condon Factors for the $IO^+(X^3\Sigma^-, a^1\Delta, b^1\Sigma^+) \leftarrow IO(X^2\Pi)$ and $IO^+(a^1\Delta, b^1\Sigma^+) \leftarrow IO^+(X^3\Sigma^-)$ Transitions Calculated Using Potential Energy Curves Obtained at the CASPT2/6-311+G(3df) Level

	v''				v''				v''			
v'	0	1	2	3	0	1	2	3	0	1	2	3
	$IO^+(X^3\Sigma^-) \leftarrow IO(X^2\Pi)$				$IO^+(a^1\Delta) \leftarrow IO(X^2\Pi)$				$IO^+(b^1\Sigma^+) \leftarrow IO(X^2\Pi)$			
0	0.61	0.31	0.07	0.01	0.80	0.18	0.02	0.00	0.98	0.02	0.00	0.00
1	0.29	0.15	0.36	0.16	0.18	0.47	0.30	0.05	0.02	0.95	0.03	0.00
2	0.08	0.31	0.01	0.29	0.02	0.27	0.24	0.37	0.00	0.03	0.91	0.05
3	0.02	0.16	0.21	0.03	0.00	0.06	0.30	0.09	0.00	0.00	0.05	0.88
	$IO^+(a^1\Delta) \leftarrow IO^+(X^3\Sigma^-)$				$IO^+(b^1\Sigma^+) \leftarrow IO^+(X^3\Sigma^-)$							
0	0.95	0.05	0.00	0.00	0.72	0.23	0.04	0.01				
1	0.05	0.85	0.09	0.01	0.24	0.31	0.31	0.10				
2	0.00	0.10	0.76	0.14	0.04	0.35	0.09	0.30				
3	0.00	0.00	0.14	0.66	0.00	0.09	0.36	0.01				

expansions.[27] The recontracted ccpvdz and sp-pvdz basis sets, as supplied with the MOLFDIR program package,[22,23] were used for oxygen and iodine, respectively. All relativistic calculations were done using the MOLFDIR package.[22,23,14]

Lacking a series of calibration calculations for which experimental values of λ_e are well-known, it is difficult to estimate the uncertainty of our estimate for IO^+. The dzp-type basis set is modest but is the largest for which the RASCI calculations were feasible. Likewise, the effect of the frozen-core approximation is unknown, although the small difference between the COSCI and RASCI predictions suggests a minor effect. Finally, the spin−spin splitting can be sensitive to errors in bond length; test COSCI calculations indicate that $d\lambda/dr$ can be as large as -1900 cm^{-1}/Å in a reasonable range of bond length r.

The great computational expense of the relativistic RASCI calculations precluded their use for directly calculating Ω-dependent bond lengths and spectroscopic constants. However, we expect the difference in bond lengths to be small based upon related molecules such as the isoelectronic TeO, for which the difference $r_e(\Omega = \pm 1) - r_e(\Omega = 0)$ is -0.003 Å.[28] The relativistic effects on calculated bond lengths in hydrogen halides and homonuclear dihalogens have been determined at various levels of theory to be rather small.[29,30]

4. Discussion

The quality of the calculations for IO^+ was assessed based on the success in reproducing the experimental results for O_2 and IO (Tables 1 and 2).

4.1. Molecular Constants. *O_2.* The CASPT2(8,6)/PBS calculations underestimate the harmonic vibrational frequency of $O_2(X^3\Sigma^-)$ by 33 cm^{-1} and overestimate the equilibrium bond length by 0.019 Å. Using the ANO basis set, the errors are +23 cm^{-1} for ω_e and -0.005 Å for r_e. Finally, using the 6-311+G(3df) basis set, the errors are +5 cm^{-1} for ω_e and +0.002 Å for r_e (Table 1).

TABLE 5. Excitation Energies (T_0) of IO^+ Calculated at the CASPT2(8,6) Level and Adiabatic Ionization Energies (IE_0) of IO Both (1) Calculated and (2) Recommended; All the Calculations Were Done with the 6-311+G(3df) Basis Set and Are Corrected for Spin−Orbit[a] and Spin−Spin[b] Splittings

state	CASPT2 T_0 (eV)	CASPT2 IE_0 (eV)	CCSD(T)+ CASPT2[c] IE_0 (eV)	recommended IE_0 (eV)
$IO(X_1^2\Pi_{3/2})$	0	0	0	0
$IO(X_2^2\Pi_{1/2})$	0.259(5)[a]			
$IO^+(X_1^3\Sigma^-_0)$	0	9.30	9.60	9.735(17)[d]
$IO^+(X_2^3\Sigma_{\pm1})$	0.13(2)[b]	9.43	9.73	9.87
$IO^+(a^1\Delta)$	0.72	10.02	10.32	10.45
$IO^+(b^1\Sigma^+)$	1.18	10.48	10.78	10.91

[a] Experimental spin−orbit splitting from refs 24 and 25. [b] Experimental spin−spin splitting derived from data in ref 4. [c] The excitation energies for the cation are calculated at the CASPT2 level and are added to the ionization energy calculated at the CCSD(T) level. [d] Experimental ionization energy from ref 4.

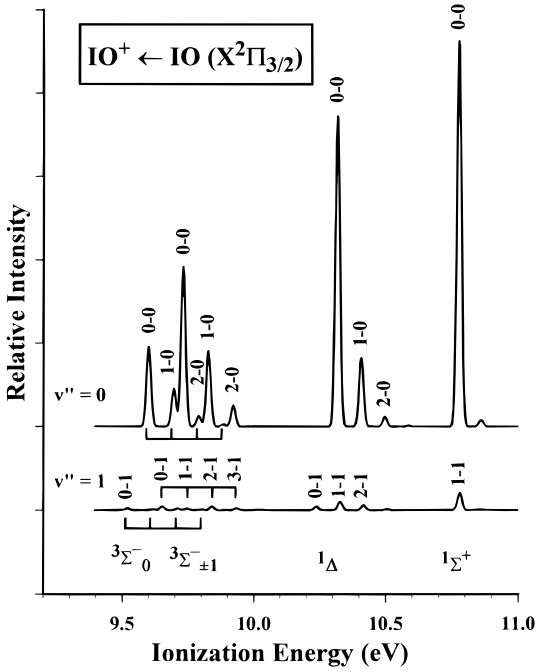

Figure 2. The simulated photoionization spectrum of IO at a spectral resolution (full width at half-maximum) of 0.02 eV. The cold ($v'' = 0$) and the hot ($v'' = 1$) bands using a temperature of 300 K are plotted on the upper and lower axes separately. The onset of ionization is from CCSD(T) calculations, and the Franck−Condon factors are from CASPT2 potential curves. Ionization to each electronic state of IO^+ was assumed equally probable.

The molecular constants calculated with the CASPT2(8,6)/6-311+G(3df) method are also in good agreement with the experimental values for the excited states (Table 1). As shown in Table 1, ω_e and B_e decrease with increasing electronic excitation while $\omega_e x_e$, D_e, and r_e increase.

Calculations at the CCSD(T)/6-311+G(3df) level yield errors of $+26$ cm^{-1} for ω_e and -0.0007 Å for r_e (O_2 $X^3\Sigma^-_g$). For both CCSD(T)/6-311+G(3df) and CASPT2(8,6)/6-311+G(3df) calculations, correlating all electrons (core not frozen) increases ω_e by 0.5% (8 cm^{-1}) and decreases r_e by 0.2% (0.002 Å).

IO. The CASPT2(9,6) energy calculations for IO failed to converge at long internuclear distances with the unmodified PBS basis set. Using the modified PBS basis set, the errors in ω_e and r_e are -34 ± 13 cm^{-1} and $+0.004 \pm 0.005$ Å as compared to the experimental Ω-averaged values of 670 ± 13 cm^{-1} (1σ) and 1.877 ± 0.005 Å (1σ), respectively. The Ω-averaged values are from the experimental values of $r_e = 1.867\,713 \pm 0.000\,046$ Å (3σ) and $\omega_e = 681.6004 \pm 0.0091$ cm^{-1} (3σ) for $IO(X^2\Pi_{3/2})$[31] and $r_e = 1.887 \pm 0.010$ Å (1σ) and $\omega_e = 658 \pm 25$ cm^{-1} (1σ) for $IO(X^2\Pi_{1/2})$.[24,25] The same method using the 6-311+G(3df) basis set has errors in ω_e and r_e of -18 ± 13 cm^{-1} and $+0.003 \pm 0.005$ Å, respectively (Table 2). Even though the CASPT2(9,6)/6-311+G(3df) calculations on IO yield good agreement with experimental values, agreement is not as good as for O_2. However, the quality of the CASPT2(8,6) results for $IO^+(X^3\Sigma^-)$ is expected to be better than CASPT2(9,6) for $IO(X^2\Pi)$ because the orbitals in the cation are more compact and therefore are better described using a radially limited basis set.

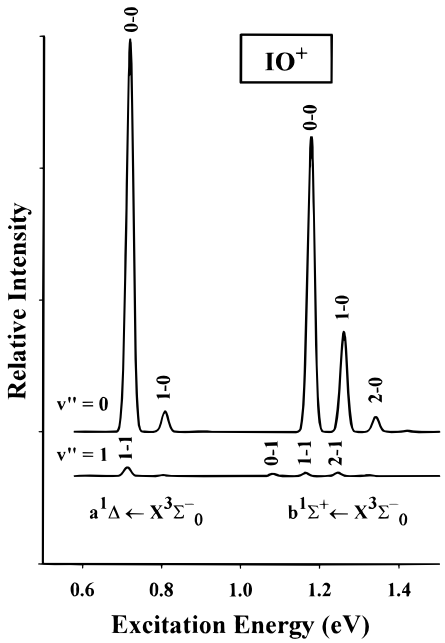

Figure 3. The simulated excitation spectrum of IO^+ at a spectral resolution (full width at half-maximum) of 0.02 eV. The cold ($v'' = 0$) and the hot bands ($v'' = 1$) using a temperature of 300 K are plotted on the upper and lower axes separately. The excitation energies and the Franck−Condon factors are from CASPT2 potential curves. Excitation to each electronically excited state of IO^+ was assumed equally probable.

The CCSD(T)/6-311+G(3df) potential yields errors in ω_e and r_e of -6 ± 13 cm^{-1} and $+0.017 \pm 0.005$ Å. A lower frequency (error $= -26 \pm 13$ cm^{-1}) and a longer bond (error $= +0.029 \pm 0.005$ Å) have been calculated by McGrath and Rowland[32] at the QCISD(T)/6-311+G(3df) level with the 4d-orbitals frozen. We repeated the QCISD(T)/6-311+G(3df) calculations including the 4d-orbitals in the correlation treatment and obtained a bond length slightly closer to the experimental value (error $= +0.020 \pm 0.005$Å).

IO^+. Based upon the above results for O_2 and IO, we concluded that the 6-311+G(3df) basis set is superior to the ANO and PBS basis sets for calculating the molecular constants and thus only the former basis set was used for IO^+.

As shown in Table 3, the trends in ω_e, B_e, $\omega_e x_e$, D_e, and r_e from the ground state to the excited states of IO^+ are similar to those observed in the isovalent molecule O_2 . The CASPT2 and CCSD(T) calculations predict $\omega_0 = 767$ and 748 cm^{-1}, respectively. Both values are much lower than a recently proposed value of $\omega_0 = 1060 \pm 160$ cm^{-1} (3σ) based on a photoionization spectrum of IO.[4] The calculated Franck-Condon intensity ratio of 2:1 for the 0−0 and 1−0 peaks (Figure 2) also disagrees with the observed intensity ratio of about 2:5.[4]

In the $XO(X^2\Pi) \leftarrow XO^-$ ($X^1\Sigma^+$) electron detachment for the series X = F, Cl, Br, and I, in which an electron is removed

from the antibonding π (π^*) orbital, ω_e increases by 37%, 28%, 25%, and 15%, respectively.[25] Apparently, the π-bonding declines from the strongly-bound FO to the weakly-bound IO. Similarly, ω_e increases by 23% from FO ($X^2\Pi$) to FO^+ ($X^3\Sigma^-$).[33−35] Thus for $IO^+ \leftarrow IO$, a small increase of 14%, obtained from our calculated value $\omega_e = 779$ cm^{-1}, is more reasonable than the 56% increase implied by the assignment in the photoionization experiment.

Furthermore, the observed spacing in the photoionization spectrum is in close agreement with our expectation for the spin−spin splitting ($2\lambda_0$) in the ground state of IO^+. A trend analysis using the isoelectronic pair Te and I^+, which have $E(^3P_1-{}^3P_2) = 4751$ and 7090 cm^{-1}, respectively,[36] and TeO ($2\lambda_0 = 679$ cm^{-1}),[28] suggests $2\lambda_0(IO^+) = 1013$ cm^{-1}. Our relativistic, multireference CI calculation predicts $2\lambda_e = 892$ cm^{-1}. The observed multiplicity ratio also agrees with the expected statistical intensity ratio of 2:1 for the transition from the ground state of the neutral to the two sublevels of the ground state of the ion, $IO^+(X^3\Sigma^-_{\pm1,0}\ v' = 0) \leftarrow IO(X^2\Pi_{3/2}\ v'' = 0)$ (Figure 2). We thus reassign the interval observed in the photoionization spectrum[4] to represent the spin−spin splitting in IO^+, $2\lambda_0 = 1060 \pm 160$ cm^{-1} (3σ).

4.2. Excitation Energies of IO^+. The calculated excitation energies for O_2 ($a^1\Delta$) ← $O_2(X^3\Sigma^-_0)$ and $O_2(b^1\Sigma^+) \leftarrow O_2$ ($X^3\Sigma^-_0$) are only 0.03 and 0.08 eV, respectively, higher than the experimental values (Table 1). The experimental excitation energies for the isovalent molecule IO^+ are not known, but a value of 0.596 eV has been suggested for the first excited state.[4] Excitation energies of 0.62 eV and 0.92 eV have also been calculated at the MCSCF level,[37] which after being corrected by zero-point vibrational energy differences (−0.003 and −0.006 eV) and the ground-state spin−spin splitting (0.13 eV), yield 0.75 and 1.04 eV, respectively. Our calculated excitation energies of 0.72 eV and 1.18 eV (Table 5) are consistent with these corrected values.

4.3. Ionization Energies. The adiabatic ionization energy of IO, corrected for the spin splittings and the zero-point vibrational energy differences, is 9.30 eV using the CASPT2/6-311+G(3df) method and is 9.60 eV using the CCSD(T)/6-311+G(3df) method. The latter value is in much better agreement with the value of 9.735 ± 0.017 eV (3σ) obtained from the photoionization experiment.[4] G2(QCI//QCI) calculations by McGrath and Rowland predicted Ω-averaged values of 9.76 ± 0.055 eV.[32] After correction for the spin−spin splitting in the ion, this yields 9.67 eV, consistent with our result.

Since both the triplet and doublet states are dominated by a single electronic configuration, CASSCF is not much superior to Hartree−Fock. However, CCSD(T) treats the dynamic electron correlation more effectively than MP2, so in this case we expect a more reliable prediction from CCSD(T) theory than from CASPT2. The ionization energies to the singlet excited states are thus expected to be more reliable if the ionization energy for the $IO^+(X^3\Sigma^-) \leftarrow IO$ ($X^2\Pi$) transition is calculated at the CCSD(T) level and added to the excitation energies of IO^+ calculated at the CASPT2(8,6) level (Table 5).

Franck−Condon factors depend primarily upon the difference in bond length between the two states (Δr_e). CCSD(T) and CASPT2 give almost the same value for $r_e(IO^+)$ but the CASPT2 result for r_e(IO) agrees better with experiment. Thus, we used the CASPT2 potential energy curves to calculate the Franck−Condon factors. This choice also maintains consistency with the potential energy curves for the singlet states, which required CASPT2 calculations.

5. Summary and Conclusions

Potential energy curves for IO($X^2\Pi$) and IO^+($X^3\Sigma^-$, $a^1\Delta$, $b^1\Sigma^+$) were computed at the CASPT2(9,6)/6-311+G(3df) and CASPT2(8,6)/6-311+G(3df) levels of theory, respectively. Potential energy curves for the ground states of the neutral and the ion, which are dominated by a single reference configuration near the equilibrium bond length, were also calculated at the CCSD(T)/6-311+G(3df) level. Seven vibrational and four rotational quantum levels were obtained by solving the rotary−vibrational Schrödinger equation numerically.[19] The molecular constants for each state were derived by fitting these levels to the formulas shown in Tables 2−3. The Franck-Condon intensities for the IO^+($X^3\Sigma^-$, $a^1\Delta$, $b^1\Sigma^+$) ← IO($X^2\Pi$) and IO^+($a^1\Delta$, $b^1\Sigma^+$) ← IO^+($X^3\Sigma^-$) transitions were calculated using the corresponding wave functions. The CCSD(T) method is superior to CASPT2 in reproducing the experimental ionization energy $IO^+(X^3\Sigma^-) \leftarrow IO(X^2\Pi)$. Since both states are dominated by a single configuration, the discrepancy between the two methods is mostly due to the dynamic electron correlation which is more effectively estimated by CCSD(T) than MP2. However, $IO^+(a^1\Delta)$ and $IO^+(b^1\Sigma^+)$ are both two-configuration states and require the multireference CASPT2 method.

An observed spacing of 1060 ± 160 cm^{-1} (3σ) in the photoionization spectrum of IO is reassigned to the spin−spin splitting rather than the vibrational frequency of the ion. The new assignment is supported by the value ω_e ($IO^+(X^3\Sigma^-)$) = 764 cm^{-1} calculated at the CCSD(T)/6-311+G(3df) level and spin−spin splitting of 892 cm^{-1} predicted by relativistic MRCISD/DZP calculations. The relative intensities of the observed bands (2:5) also agree better with the statistical intensity ratio of 1:2 expected for the two sublevels of the ground state of the ion ($X^3\Sigma^-_{0,\pm1}$) than with the Franck-Condon intensity ratio of 2:1 corresponding to the vibrational assignment ($X^3\Sigma^-_0$, $v = 0,1$).

As observed in the isovalent O_2 molecule, the bond length of IO^+ increases and the vibrational frequency decreases with increasing electronic excitation.

Acknowledgment. We are grateful to Bert de Jong for providing the MOLFDIR program package to us and for essential advice on the relativistic calculations.

References and Notes

(1) Solomon, S.; Garcia, R. R.; Ravishankara, A. R. *J. Geophys. Res.* **1994**, *99D*, 20491−20499.
(2) Solomon, S.; Burkholder, J. B.; Ravishankara, A. R.; Garcia, R. R. *J. Geophys. Res.* **1994**, *99D*, 20929−20935.
(3) Daykin, E. P.; Wine, P. H. *J. Phys. Chem.* **1990**, *94*, 4528−4535.
(4) Zhang, Z.; Monks, P. S.; Stief, L. J.; Liebman, J. F.; Huie, R. E.; Kuo, S.-C.; Klemm, R. B. *J. Phys. Chem.* **1996**, *100*, 63−68.
(5) Hassanzadeh, P.; Irikura, K. K. *J. Phys. Chem. A* **1997**, *101*, 1580−1587.
(6) Purvis, G. D.; Bartlett, R. J. *J. Chem. Phys.* **1982**, *76*, 1910.
(7) Scuseria, G. E.; Janssen, C. L.; Schaefer, H. F., III *J. Chem Phys.* **1988**, *89*, 7382.
(8) Scuseria, G. E.; Schaefer, H. F., III *J. Chem. Phys.* **1989**, *90*, 3700.
(9) Pople, J. A.; Head-Gordon, M.; Raghavachari, K. *J. Chem. Phys.* **1987**, *87*, 5968−5975.
(10) Gauss, J.; Cremer, C. *Chem. Phys. Lett.* **1988**, *150*, 280.
(11) Salter, E. A.; Trucks, G. W.; Bartlett, R. J. *J. Chem. Phys.* **1989**, *90*, 1752.
(12) Andersson, K.; Malmqvist, P.-Å.; Roos, B. O. *J. Chem. Phys.* **1992**, *96*, 1218−1226.
(13) Frisch, M. J.; Trucks, G. W.; Schlegel, H. B.; Gill, P. M. W.; Johnson, B. G.; Robb, M. A.; Cheeseman, J. R.; Keith, T.; Petersson, G. A.; Montgomery, J. A.; Raghavachari, K.; Al-Laham, M. A.; Zakrzewski, V. G.; Ortiz, J. V.; Foresman, J. B.; Cioslowski, J.; Stefanov, B. B.; Nanayakkara, A.; Challacombe, M.; Peng, C. Y.; Ayala, P. Y.; Chen, W.; Wong, M. W.; Andres, J. L.; Replogle, E. S.; Gomperts, R.; Martin, R. L.; Fox, D. J.; Binkley, J. S.; Defrees, D. J.; Baker, J.; Stewart, J. P.; Head-

Gordon, M.; Gonzalez, C.; Pople, J. A. Gaussian 94; Gaussian, Inc.: Pittsburgh, PA, 1995.

(14) Certain commercial materials and equipment are identified in this paper in order to specify procedures completely. In no case does such identification imply recommendation or endorsement by the National Institute of Standards and Technology, nor does it imply that the material or equipment identified is necessarily the best available for the purpose.

(15) Glukhovtsev, M. N.; Pross, A.; McGrath, M. P.; Radom, L. *J. Chem. Phys.* **1995**, *103*, 1878−1885.

(16) Sadlej, A. J. *Collect. Czech. Chem. Commun.* **1988**, *53*, 1995−2016.

(17) Sadlej, A. J. *Theor. Chim. Acta* **1991**, *79*, 123−140.

(18) Sadlej, A. J. *Theor. Chim. Acta* **1992**, *81*, 339−354.

(19) Andersson, K.; Blomberg, M. R. A.; Fülscher, M. P.; Karlström, G.; Kellö, V.; Lindh, R.; Malmqvist, P.-Å.; Noga, J.; Olsen, J.; Roos, B. O.; Sadlej, A. J.; Siegbahn, P. E. M.; Urban, M.; Widmark, P.-O. MOLCAS, Version 3. University of Lund, Sweden, 1994.

(20) ACES II, an ab initio program system authored by J. F. Stanton, J. Gauss, J. D. Watts, W. J. Lauderdale, and R. J. Bartlett. The package also contains modified versions of the MOLECULE Gaussian integral program of J. Almlöf and P. R. Taylor, the ABACUS integral derivative program of T. U. Helgaker, H. J. A. Jense, P. Jorgensen, and P. R. Taylor, and the PROPS property integral package of P. R. Taylor.

(21) Stanton, J. F.; Gauss, J.; Watts, J. D.; Lauderdale, W. J.; Bartlett, R. J. *Int. J. Quantum. Chem.* **1992**, *S26*, 879−894.

(22) (a) Aerts, P. J. C.; Visser, O.; Visscher, L.; Merenga, H.; de Jong, W. A.; Nieuwpoort, W. C. *MOLFDIR;* University of Groningen, The Netherlands. (b) For a description of, as well as ordering instructions for, MOLFDIR, see: World Wide Web home page, http://theochem.chem.rug.nl/~bert/Molfdir/Molfdir.html.

(23) Visscher, L.; Visser, O.; Aerts, P. J. C.; Merenga, H.; Nieuwpoort, W. C. *Comput. Phys. Commun.* **1994**, *81*, 120−144.

(24) Gilles, M. K.; Polak, M. L.; Lineberger, W. C. *J. Chem. Phys.* **1991**, *95*, 4723−4724.

(25) Gilles, M. K.; Polak, M. L.; Lineberger, W. C. *J. Chem. Phys.* **1992**, *96*, 8012−8020.

(26) Olsen, J.; Roos, B. O.; Jørgensen, P.; Jensen, H. J. A. *J. Chem. Phys.* **1988**, *89*, 2185−2192.

(27) Visser, O.; Visscher, L.; Aerts, P. J. C.; Nieuwpoort, W. C. *J. Chem. Phys.* **1992**, *96*, 2910−2919.

(28) Huber, K. P.; Herzberg, G. *Molecular Spectra and Molecular Structure: IV. Constants of Diatomic Molecules*; van Nostrand Reinhold: New York, 1979.

(29) Visscher, L.; Dyall, K. G. *J. Chem. Phys.* **1996**, *104*, 9040−9046.

(30) Visscher, L.; Dyall, K. G. *J. Chem. Phys.* **1996**, *105*, 1987−1994.

(31) Bekooy, J. P.; Meerts, W. L.; Dymanus, A. *J. Mol. Spectrosc.* **1983**, *102*, 320−343.

(32) McGrath, M. P.; Rowland, F. S. *J. Phys. Chem.* **1996**, *100*, 4815−4822.

(33) Hammer, P. D.; Sinha, A.; Burkholder, J. B.; Howard, C. J. *J. Mol. Spectrosc.* **1988**, *129*, 99−118.

(34) Dyke, J. M.; Jonathan, N.; Mills, J. D.; Morris, A. *Mol. Phys.* **1980**, *40*, 1177.

(35) Johnson, R. D., III *Chem. Phys. Lett.* **1995**, *245*, 484−487.

(36) Moore, C. E. *Atomic Energy Levels*; U.S. Government Printing Office: Washington, DC, 1971.

(37) M. Krauss, personal communication cited in ref. 4.